Mem. S.A.It. Vol. 79, 552

Memorie della

Measuring stellar mass loss in different environments

Jasonjot S. Kalirai[1,2]

[1] University of California Observatories/Lick Observatory, University of California at Santa Cruz, 1156 High Street, Santa Cruz CA, 95060 e-mail: jkalirai@ucolick.org
[2] Hubble Fellow

Abstract. We present deep imaging (CFHT/CFH12K) and spectroscopic (Keck/LRIS) observations of white dwarfs in three rich open star clusters that span a wide range in both age (t = 1.4 Gyr – 8.5 Gyr) and metallicity (Z = 0.014 – 0.043), NGC 7789, NGC 6819, and NGC 6791. Masses for the remnant white dwarfs in each cluster are measured and linked to their progenitor star masses to yield a new initial-final mass relation. We explore the total integrated stellar mass loss as a function of environment and find that Solar metallicity stars with $M_{\rm initial}$ = 1.5 – 2.0 $M_{\odot}$ will lose ~65 – 70% of their mass through post main-sequence evolution. For the case of the most metal-rich open star cluster, NGC 6791 (2.5× $Z_{\odot}$), the mean mass of the white dwarfs is measured to be very low, 0.43 $M_{\odot}$. This suggests that the rate of mass loss is enhanced in post main-sequence evolutionary phases (such as the red giant branch) for higher metallicity stars. These results naturally explain both the presence of extreme horizontal branch stars in NGC 6791 and the recent finding of an anomalously low white dwarf cooling age for this cluster.

Key words. open clusters and associations: individual (NGC 7789, NGC 6819, and NGC 6791) - stars: evolution - techniques: photometric, spectroscopic - white dwarfs

1. Introduction

The initial-final mass relation denotes a mapping from the initial mass of a main-sequence star to its final white dwarf configuration and hence provides the total mass loss that a star has undergone through its lifetime, a fundamental property of stellar evolution (Reimers 1975; Renzini & Fusi Pecci 1988; Weidemann 2000). Most of the mass loss that a star suffers through its evolution occurs during very short lived post-main-sequence evolutionary phases such as the red giant branch, asymptotic giant branch, and planetary nebula phases (e.g., see Reimers 1975). Theoretically, the relation is poorly constrained given the difficulty in understanding mass loss mechanisms such as thermal pulses on the asymptotic giant branch (Weidemann 2000; Marigo 2001; also see Habing 1996 for a review). Direct observational constraints are rare as the lifetimes of stars in these phases are short (~10^5 years) and the stars themselves are usually obscured by dusty shells.

An alternate method to measure the relation comes from the study of white dwarfs in star clusters and binary systems. Spectroscopic observations of these remnant stars can yield their masses through Balmer line fit-

Send offprint requests to: J. Kalirai

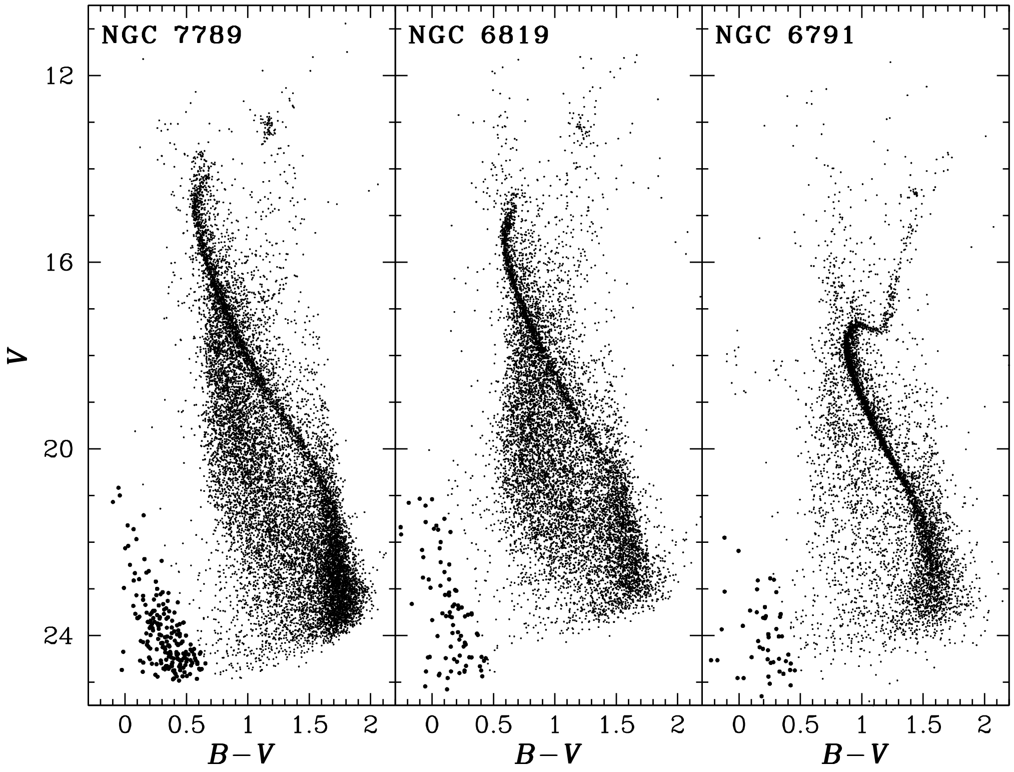

Fig. 1. CFHT/CFH12K color-magnitude diagrams of NGC 7789 (t = 1.4 Gyr), NGC 6819 (t = 2.5 Gyr), and NGC 6791 (t = 8.5 Gyr) clearly show well defined main-sequences and post main-sequence evolutionary phases. A large number of white dwarf candidates are also evident in the faint blue part of the diagrams (larger dots).

ting (Bergeron, Saffer, & Liebert 1992). With knowledge of the system's total age (i.e., cluster age), the progenitor mass of the star that produced the remnant can be calculated (e.g., Weidemann 2000). This method has been successfully used to populate the high mass end of the initial-final mass relation through a series of studies by D. Koester and D. Reimers over the past 30 years (see Weidemann 2000 and references therein). More recently, several groups have built on these initial studies and more than doubled the existing sample of data points (Claver et al. 2001; Dobbie et al. 2004, 2006; Williams, Bolte, & Koester 2004; Kalirai et al. 2005; Liebert et al. 2005; Williams & Bolte 2007). In general, the initial-final mass relation shows a trend whereby more massive main-sequence stars produce more massive white dwarfs. Despite the wealth of data that has been collected to constrain this fundamental relation, current data still only exists for mostly Solar metallicity stars with $M_{\rm initial} \gtrsim 2.75~M_{\odot}$. This lower limit represents the turnoff mass of the oldest clusters in which direct white dwarf mass measurements exist (e.g., the Hyades and Praesepe systems). In this paper, we extend these mass measurements to white dwarfs in three much older clusters, with turnoff masses as low as $\sim$1 $M_{\odot}$.

2. Photometric and spectroscopic observations

We imaged NGC 7789, NGC 6819, and NGC 6791 with the CFH12K mosaic CCD camera on the 4-meter Canada-France-Hawaii Telescope (CFHT) as a part of the CFHT Open Star Cluster Survey (Kalirai et al. 2001a). The camera contains 12 CCDs, each with 2048 × 4096 pixels (a total of over 100 million pixels), at an individual pixel scale of $0\farcs206$. The projection on the sky is $42' \times 28'$ and therefore the dominant population of all three clusters is probed out to near the tidal radii. The observations were taken in the V and B filters, down to a limiting magnitude of $V \sim 25$ to ensure a solid detection of the white dwarf cooling sequence in each cluster. The data reduction methods for the NGC 6819 data are described in Kalirai et al. (2001a,b), NGC 6791 in Kalirai et al. (2007a), and NGC 7789 in Kalirai et al. (2007b).

The CFHT photometry/astrometry of the white dwarfs in each cluster was used as input to create Keck/LRIS multi-object spectroscopic masks. These were observed on the Keck I telescope in July and August 2005. The field of view of the spectrograph ($5' \times 7'$) is much smaller than the wide-field imaging data and so the field was positioned to include as many of the bright white dwarf candidates as possible. We used the 600/4000 grism (dispersion = 0.63 Å/pixel) which simultaneously covers 2580 Å, from 3300 – 5880 Å, ensuring a spectral range that includes hydrogen Balmer lines from Hβ to higher order lines such as H10. The spectroscopic data reduction are described in Kalirai et al. (2007a) and Kalirai et al. (2007b).

3. Color-magnitude diagrams

We present the cluster color-magnitude diagrams for each of NGC 7789, NGC 6819, and NGC 6791 in Figure 1. The main sequence of each cluster can be cleanly traced from low mass stars at $V \sim 23 – 24$ up to the turnoff. Post main-sequence phases, such as the red giant branch and red giant clump are also evident. The white dwarf cooling sequences of both NGC 7789 and NGC 6819 are clearly visible in the faint-blue part of the CMDs, whereas a number of bright white dwarf candidates appear to be detected in NGC 6791 (these points have been made larger for clarity).

As discussed in Kalirai et al. (2007a) and Kalirai et al. (2007b), we can use these data, combined with reddening and metallicity estimates from the literature, to independently measure the fundamental parameters of each cluster. The distances are measured by fitting the observed data to the Hyades cluster main-sequence, and the ages are estimated by comparing to stellar isochrones from VandenBerg, Bergbusch, & Dowler (2006). We find that NGC 7789 has $(m - M)_V = 12.5 \pm 0.1$, $Z = 0.014$, and $t = 1.4$ Gyr. For NGC 6819, we find $(m - M)_V = 12.30 \pm 0.12$, $Z = 0.017$, and $t = 2.5$ Gyr. Finally, for NGC 6791 we find $(m - M)_V = 13.43 \pm 0.10$, $Z = 0.043$, and $t = 8.5$ Gyr.

Given the older ages of these three clusters, the turnoff masses are 2.0, 1.6, and 1.1 $M_\odot$, respectively, and therefore the bright cluster white dwarfs must have evolved from stars just above these masses. As we show below, there are currently no direct observational constraints on the amount of stellar mass loss that such stars suffer through their evolution.

4. White dwarf mass measurements and the initial-final mass relation

For NGC 7789, NGC 6819, and NGC 6791, we targeted 15, 14, and 13 candidates for spectroscopy, respectively. Of these, 14, 8, and 12 of the targets are confirmed as white dwarfs, the rest being either background galaxies or distant field main-sequence stars. Although we can classify each of these stars, we can not spectroscopically measure a mass for the fainter targets in our sample given the noisier spectra. These mass measurements require both lower and higher order Balmer lines to be well characterized as discussed in Bergeron, Saffer, & Liebert (1992) and Bergeron, Liebert, & Fulbright (1995). Our spectra yield mass measurements for 6 stars in NGC 7789, 4 stars in NGC 6819, and 12 stars in NGC 6791.

The mean masses of the *cluster member* white dwarfs in this sample are found to be $M_{\rm final}$ = 0.61 ± 0.02 $M_\odot$ in NGC 7789, $M_{\rm final}$ = 0.54 ± 0.01 $M_\odot$ in NGC 6819, and $M_{\rm final}$ = 0.43 ± 0.06 $M_\odot$ in NGC 6791. Remarkably, the mean mass of NGC 6791's white dwarf population is less than the critical mass at which helium ignites in the core of the progenitor star (~0.47 $M_\odot$ for this metallicity, Dominguez et al. 1999; Pietrinferni et al. 2004), and therefore some of these white dwarfs must be helium core stars. As predicted by Hansen (2005), such evolution in this cluster would explain the anonalously low cluster white dwarf cooling age of 2.4 Gyr determined by Bedin et al. (2005) since helium core white dwarfs cool a factor of ~3× slower than carbon-oxygen core white dwarfs. The progenitors of these stars evolved through a unique channel in which they "peeled" off of the red giant branch before experiencing a helium flash due to enhanced mass loss, most likely driven by the extrememly high metallicity of the cluster. This scenario was first predicted by Faulkner 1972 to explain the extreme horizontal branch stars (note, this cluster is the only open cluster to contain a substantial population of these stars) and later expanded in Castellani & Castellani (1993). As discussed in Kalirai et al. (2007a), we estimate that the birthrate of these helium core white dwarfs in NGC 6791 is between 40 – 70%.

Of the dozen white dwarfs with mass measurements in the NGC 6791 data set, it appears only two of them could have formed from the canonical evolutionary channel involving a helium flash at the tip of the red giant branch. To be conservative, we only consider the one star with $M_{\rm final}$ = 0.53 ± 0.02 $M_\odot$ which must be a carbon-oxygen core white dwarf. We place this point, as well as the results for NGC 7789 and NGC 6819, on the initial-final mass relation in Figure 2 (top). Clearly, the general trend at higher masses (crosses) continues down to stars with masses similar to the Sun. In the bottom panel, we plot the total integrated stellar mass loss as a function of initial mass. For the most massive main-sequence stars that will form white dwarfs, this yield is about ~85%. A slightly less massive star such as the progenitor

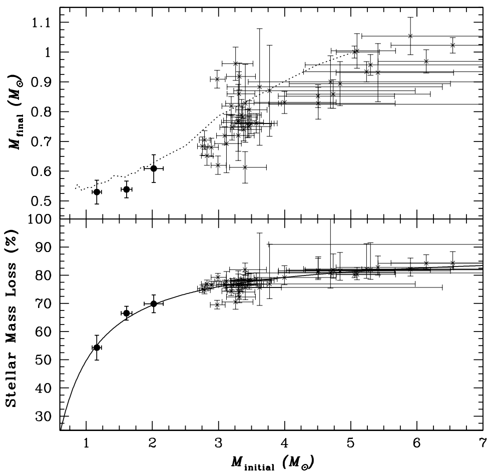

Fig. 2. *Top* – The initial-final mass relation including all previous data (crosses) and the results from NGC 7789, NGC 6819, and NGC 6791 (larger data points). For these clusters, we have binned all white dwarfs in a given cluster and plotted a single data point indicating the weighted mean mass and 2σ uncertainty in the mean. The dotted curve indicates the theoretical initial-final mass relation from Marigo (2001) for Solar metallicity. *Bottom* – The total integrated stellar mass as a function of initial mass, along with our best fit linear relation.

of Sirius B (5.06 $M_\odot$ – Liebert et al. 2005) has lost 80% of its mass. The mass loss smoothly decreases with stellar mass down to ~75% for intermediate mass stars, 3 < $M_{\rm initial}$ < 4 $M_\odot$. Our new data points suggest a more rapid decline for stars with $M \lesssim 2$ $M_\odot$. At this mass, stars will lose ~70% of their total mass however this decreases down to just ~55% for stars approximately the mass of the Sun.

5. Conclusions

The direct measurement of white dwarf masses in well studied clusters with ages 1 – 8 Gyr have provided the first constraints on the low mass end of the initial-final mass relation. This has several important implications. The extension of the relation represents a four fold increase in the total number of hydrogen burning stars for which the integrated mass loss can now be calculated from empirical data, assuming a Salpeter initial mass function. The new relation can be combined with white dwarf luminosity function measurements in the Galactic disk and halo to yield the ages of these components (e.g., Ferrario et al. 2005 and Hansen et al. 2007). The relation also serves as a key input to chemical evolution models of galaxies and therefore enhances our understanding of star formation efficiencies in these systems (Somerville & Primack 1999). A linear parameterization of the current data points suggests that $M_{\rm final} = (0.109 \pm 0.007)\ M_{\rm initial} + 0.394 \pm 0.025\ M_\odot$ (solid curve in Figure 2).

Acknowledgements. Data presented in this article were obtained at both the W. M. Keck Observatory and the Canada-France-Hawaii Telescope (CFHT). I wish to thank several people who helped shape this article, P. Bergeron, B. Hansen, D. Kelson, D. Reitzel, R. Rich, H. Richer, J. Liebert, R. Eakin, D. Vandenberg, and L. Girardi. Support for this work was provided by Hubble Fellowship grant HF-01185.01-A and NASA/STScI grant HST-GO-10424.

References

Bedin, L. R., Salaris, M., Piotto, G., King, I. R., Anderson, J., Cassisi, S., & Momany, Y. 2005, ApJ, 624, L45
Bergeron, P., Saffer, R. A., & Liebert, J. 1992, ApJ, 394, 228
Bergeron, P., Liebert, J., & Fulbright, M. S. 1995, AJ, 444, 810
Castellani, M., & Castellani, V. 1993, ApJ, 407, 649
Claver, C. F., Liebert, J., Bergeron, P., & Koester, D. 2001, ApJ, 563, 987
Dobbie, P. D., Pinfield, D. J., Napiwotzki, R., Hambly, N. C., Burleigh, M. R., Barstow, M. A., Jameson, R. F., & Hubeny, I. 2004, MNRAS, 355, L39
Dobbie, P. D., et al. 2006, MNRAS, 369, 383
Dominguez, I., Chieffi, A., Limongi, M., & Straniero, O. 1999, ApJ, 524, 226
Faulkner, J. 1972, ApJ, 172, 401
Ferrario, L., Wickramasinghe, D., Liebert, J., & Williams, K. A. 2005, MNRAS, 361, 1131
Habing, H. J. 1996, ARA&A, 7, 97
Hansen, B. M. S. 2005, ApJ, 635, 522
Hansen, B. M. S., et al. 2007, ApJ in press, (astro-ph/071738)
Kalirai, J. S., Richer, H. B., Fahlman, G. G., Cuillandre, J., Ventura, P., D'Antona, F., Bertin, E., Marconi, G. & Durrell, P. 2001a, AJ, 122, 257
Kalirai, J. S., Richer, H. B., Fahlman, G. G., Cuillandre, J., Ventura, P., D'Antona, F., Bertin, E., Marconi, G. & Durrell, P. 2001b, AJ, 122, 266
Kalirai, J. S., Richer, H. B., Reitzel, D., Hansen, B. M. S., Rich, R. M., Fahlman, G. G., Gibson, B. K., & von Hippel, T. 2005, ApJ, 618, L123
Kalirai, J. S., Bergeron, P., Hansen, B. M. S., Kelson, D. D., Reitzel, D. B., Rich, R. M., & Richer, H. B. 2007a, ApJ in press (astro-ph/0705.0977)
Kalirai, J. S., Hansen, B. M. S., Kelson, D. D., Reitzel, D. B., Rich, R. M., & Richer, H. B. 2007b, ApJ submitted (astro-ph/0706.3894)
Liebert, J., Young, P. A., Arnett, D., Holberg, J. B., & Williams, K. A. 2005, ApJ, 630, L69
Marigo, P. 2001, A&A, 370, 194
Pietrinferni, A., Cassisi, S., Salaris, M., & Castelli, F. 2004, ApJ, 612, 168
Reimers, D. 1975, Societe Royale des Sciences de Liege, Memoires, 8, 369
Renzini, A., & Fusi Pecci, F. 1988, ARA&A, 26, 199
Somerville, R. S., & Primack, J. R. 1999, MNRAS, 310, 1087
VandenBerg, D. A., Bergbusch, P. A., & Dowler, P. D. 2006, ApJS, 162, 375
Weidemann, V. 2000, A&A, 363, 647
Williams, K. A., Bolte, M., & Koester, D. 2004, ApJ, 615, L49
Williams, K. A., & Bolte, M. 2007, AJ, 133, 1490